HAL
open science

Prolongation of the lifetime of guided discharges triggered in atmospheric air by femtosecond laser filaments up to 130 μs

Leonid Arantchouk, B. Honnorat, E. Thouin, G. Point, A. Mysyrowicz, Aurélien Houard

To cite this version:

Leonid Arantchouk, B. Honnorat, E. Thouin, G. Point, A. Mysyrowicz, et al.. Prolongation of the lifetime of guided discharges triggered in atmospheric air by femtosecond laser filaments up to 130 μs. Applied Physics Letters, 2016, 108 (17), pp.173501 10.1063/1.4947273 . hal-01314451v1

HAL Id: hal-01314451

https://hal.sorbonne-universite.fr/hal-01314451v1

Submitted on 11 May 2016 (v1), last revised 18 May 2016 (v2)

HAL is a multi-disciplinary open access archive for the deposit and dissemination of scientific research documents, whether they are published or not. The documents may come from teaching and research institutions in France or abroad, or from public or private research centers.

L'archive ouverte pluridisciplinaire **HAL**, est destinée au dépôt et à la diffusion de documents scientifiques de niveau recherche, publiés ou non, émanant des établissements d'enseignement et de recherche français ou étrangers, des laboratoires publics ou privés.

AIP Applied Physics Letters

Prolongation of the lifetime of guided discharges triggered in atmospheric air by femtosecond laser filaments up to 130 μs

L. Arantchouk, B. Honnorat, E. Thouin, G. Point, A. Mysyrowicz, and A. Houard

Citation: Applied Physics Letters **108**, 173501 (2016); doi: 10.1063/1.4947273
View online: http://dx.doi.org/10.1063/1.4947273
View Table of Contents: http://scitation.aip.org/content/aip/journal/apl/108/17?ver=pdfcov
Published by the AIP Publishing

Articles you may be interested in

Tesla coil discharges guided by femtosecond laser filaments in air
Appl. Phys. Lett. **100**, 181112 (2012); 10.1063/1.4711208

Triggering, guiding and deviation of long air spark discharges with femtosecond laser filament
AIP Advances **2**, 012151 (2012); 10.1063/1.3690961

Improved laser triggering and guiding of meqavolt discharges with dual fs-ns pulses
Appl. Phys. Lett. **88**, 021101 (2006); 10.1063/1.2162430

Measurements of intense femtosecond laser pulse propagation in aira)
Phys. Plasmas **12**, 056705 (2005); 10.1063/1.1871197

Streamerless guided electric discharges triggered by femtosecond laser filaments
Phys. Plasmas **10**, 4530 (2003); 10.1063/1.1618776

Reuse of AIP Publishing content is subject to the terms at: https://publishing.aip.org/authors/rights-and-permissions. Download to IP: 134.157.80.70 On: Mon, 09 May 2016 08:45:08

Prolongation of the lifetime of guided discharges triggered in atmospheric air by femtosecond laser filaments up to 130 μs

L. Arantchouk,[1,2,a)] B. Honnorat,[1] E. Thouin,[1] G. Point,[1] A. Mysyrowicz,[1] and A. Houard[1]
[1]*LOA, ENSTA ParisTech, CNRS, Ecole Polytechnique, Université Paris-Saclay, 828 bd des Maréchaux, 91762 Palaiseau Cedex, France*
[2]*Laboratoire de Physique des Plasmas, CNRS, Ecole Polytechnique, UPMC, Université Paris-Sud, 91128 Palaiseau, France*

(Received 19 February 2016; accepted 4 April 2016; published online 25 April 2016)

The triggering and guiding of electric discharges produced in atmospheric air by a compact 100 kV Marx generator is realized in laboratory using an intense femtosecond laser pulse undergoing filamentation. We describe here an approach allowing extending the lifetime of the discharges by injecting a current with an additional circuit. Laser guiding discharges with a length of 8.5 cm and duration of 130 μs were obtained. *Published by AIP Publishing.*
[http://dx.doi.org/10.1063/1.4947273]

In the last decade, femtosecond laser filaments have proved to be a powerful tool to trigger and guide electric discharges in atmospheric air[1] with gap length of a few meters.[2–6] The weakly ionized plasma column and subsequent low density channel generated by laser filaments allow the precise triggering and guiding of electric discharges between two electrodes with a significant reduction of the breakdown voltage.[7–9] This effect is potentially useful for the development of laser lightning rod,[4,10,11] high-voltage, high-current switches,[12] or virtual plasma antennas.[13,14]

For applications such as plasma antennas, extension of the filament plasma lifetime is needed, since the plasma from the filament recombines in a few nanoseconds, seriously limiting the bandwidth of antennas to frequencies $v > 10^9$ Hz. This can be done using additional femtosecond or nanosecond laser pulses,[15–17] but this technique is particularly complex and the resulting plasma is limited to a few μs. Injection of electric current through guided discharges appears to be a more promising way. The duration of the guided discharge mostly depends on the high voltage (HV) source, with a typical duration on the order of 100 ns.[2–4,14] In several publications, a Marx generator was used as the HV source to produce meter scale guided discharges. In this case, the discharge duration is defined by the product of the Marx "stack" capacitance C_{marx} and a discharge load R_{load}. In Ref. 18, a compact Marx generator was used to create a ~21 cm guided discharge of duration about 600 ns due to the mentioned Marx capacitance $C_{max} \sim 2$ nF and the discharge load resistance $R_d \sim 300\,\Omega$. In this letter, we describe a method, which allows prolonging this parameter up to 130 μs.

The experimental setup is presented in Fig. 1. The circuit is composed of two parts. The first part is a Marx generator described in Ref. 18. For this experiment, the generator was composed of 5 stages charged up to 20 kV DC, resulting in 100 kV output pulse with a negative polarity. An inductance L_1 was connected to the generator output electrode and served as a load up to the moment when the Marx pulse produces a breakdown in the inter-electrode gap. The Marx output electrode has a cylinder form with an axial hole allowing the laser beam to enter in the generator and to trigger it. The second electrode is a round finger with a 5 mm radius. As described in Ref. 18, a chirped pulse amplified laser system emitting at a wavelength of 800 nm is used to produce the filaments between the two electrodes and inside the Marx generator. The laser pulse with energy of 200 mJ, pulse duration of 700 fs, and diameter of 30 mm FWHM is focused by a convex lens (focal f = 5 m), generating a bundle of plasma channels over 1.5 m before the geometrical focus of the lens (see characterization of the filament bundle in Ref. 19). The geometrical focus of the beam was positioned 30 cm after the Marx entrance electrode in order to trigger the Marx generator as well as the guided discharge.

The second part of the circuit consists of a capacitor C_2, a resistor R_2, and an inductance L_2. To create a polarity regime, the capacitor is charge up to ±20 kV DC. The circuit is operating as follows. The laser passes first between the two electrodes and then enters into the Marx generator from its output side. This configuration gives the shortest delay

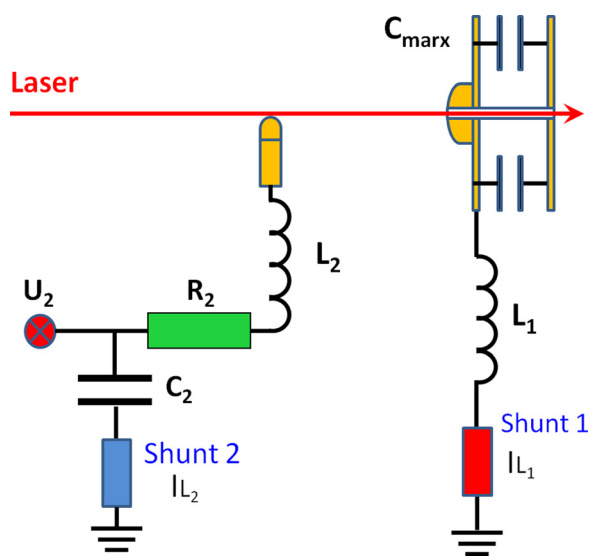

FIG. 1. Schematic view of the experimental set-up with a HV source (Marx generator) and an additional circuit $R_2L_2C_2$.

a)Author to whom correspondence should be addressed. Electronic mail: leonid.arantchouk@lpp.polytechnique.fr.

Reuse of AIP Publishing content is subject to the terms at: https://publishing.aip.org/authors/rights-and-permissions. Download to IP: 134.157.80.70 On: Mon, 09 May 2016 08:45:08

between the HV Marx pulse and the gap breakdown.[18] The breakdown generates a plasma column between the electrodes, which makes possible discharging the capacitor C_2 through L_2, R_2, and L_1. There is almost no current from the capacitor C_2 discharging through the Marx because of well matched parameters of the circuit. Thus a current is injected in the plasma channel prepared by the HV charged source with help of the low voltage charged circuit.

The operation of the circuit is monitored by means of two shunts. The first one measures the current I_{L1} flowing through the coil L_1, while the second shunt measures the current I_{L2} flowing through the coil L_2.

To demonstrate the proposed method, a minimal duration of 130 μs has been chosen for the discharge. Based on the previous study with the Marx generator,[18] we chose parameters of the circuit producing an "effective" electric field $U_{marx}/L > 10$ kV/cm with a breakdown delay smaller than 300–400 ns (where U_{marx} is the Marx output voltage and L is the gap length). Therefore, we started the experiments with a gap $L = 85$ mm and an inductance $L_1 > 400\,\mu$H, which provides no more than 5% drop of the output Marx voltage during the breakdown delay. To inject the Marx discharge into the 85 mm gap, we need $L_2 \ll L_1$, while the protection of the capacitor C_2 from the Marx 100 kV pulse brings the condition $C_2 \gg C_{marx}$. To fulfill these conditions, the following circuit parameters were chosen: $L_2 = 29\,\mu$H, $C_2 = 37$ nF, and $L_1 = 404\,\mu$H.

Typical experimental signals of the currents I_{L1} and I_{L2} are shown in Fig. 2 in the case of oscillating regime with a small resistance R_2. Two cases are presented here: (a) without any polarization: only high frequency oscillations (HF) defined by the circuit C_{marx}-L_2-R_2-C_2 are observed. Their period is $T(HF) \approx 2\pi\,(C_{marx} \times L2)^{0.5} = 1.6\,\mu$s, and the amplitude of the first current peak is about 600 A. In this case, effective discharge duration is about 10 μs. (b) The capacitor C_2 is charge negatively up to $U_{C2} = -20$ kV. In this case, the low frequency (LF) oscillations with period $T(LF) \approx 2\pi\,(C2 \times L1)^{0.5} \approx 25\,\mu$s produced by the circuit C_2-L_2-L_1 become the most pronounced. When a negative polarization U_2 is applied, the breakdown voltage reaches 80 kV, while in the case of positive polarization, it reaches 120 kV. As a consequence, the breakdown delay decreases from 210 ± 45 ns to 148 ± 21 ns when the polarity is changed. The current amplitude also depends on the applied polarity U_2. The regime of the negative polarization produces smaller HF amplitude ($I_{peak} = -390$ A for $U_{C2} = -20$ kV against $I_{peak} = -750$ A for $U_{C2} = 20$ kV) and higher LF amplitude ($I_{peak} = -220$ A for $U_{C2} = -20$ kV against $I_{peak} = 135$ A for $U_{C2} = 20$ kV). Due to the LF current injection, the effective discharge duration becomes longer than 100 μs. Note, in Fig. 2(c), that the LF currents I_{L1} and I_{L2} are opposite but with the same amplitudes, meaning that the LF current circulates inside the same circuit loop.

The resistance R_2 allows changing the damping factor of the circuit. To obtain an alternative regime, we used $R_2 = 10\,\Omega$, which is much smaller than the impedances of HF and LF circuits $\sim 110\,\Omega$. A fitting of the current signals considering a damped sinusoidal function allows one to determine the total discharge resistance R_{disch} and the circuit parameters. The total resistance varies in the range between $16\,\Omega$ and $23\,\Omega$ depending on experiment series. These values

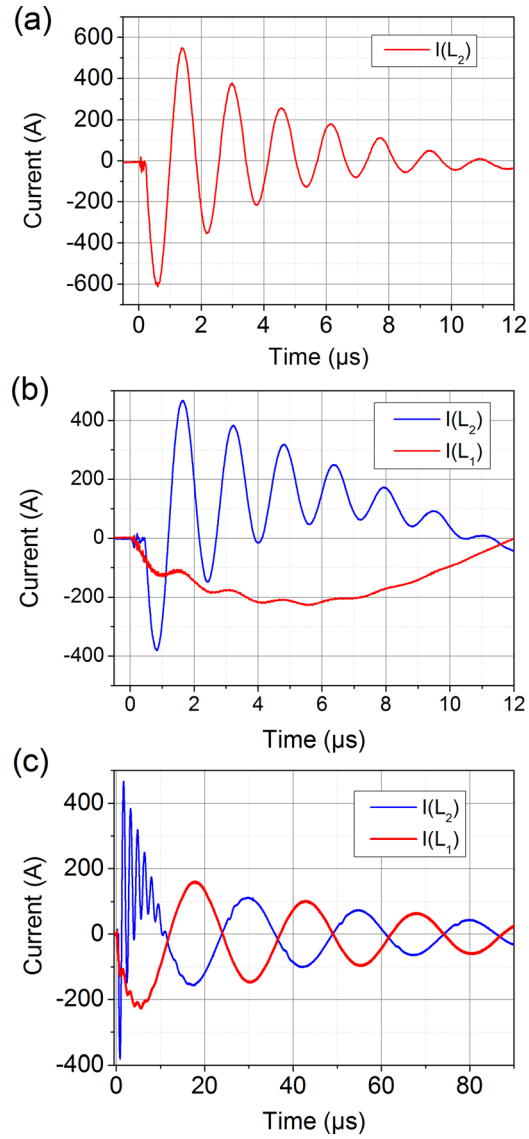

FIG. 2. Current signals I_{L1} and I_{L2} with $R_2 = 10\,\Omega$: (a) without any polarization: I_{max} (HF) ≈ -600 A; I_{max} (BF) ≈ -45 A; (b) $U_{C2} = -20$ kV: two first HF peaks are I_{max} (HF) ≈ -390 A and I_{max} (HF) ≈ 470 A. I_{peak} (BF) ≈ -220 A.

exceed the resistance $R_2 = 10\,\Omega$. Measurements with different gap lengths L in the range of 15–85 mm revealed that R_{disch} does not depend on this gap length. It means that the measured guided discharge resistance is mostly due to some contact processes in the vicinity of the electrodes. It is also interesting to note that R_{disch} remains remarkably constant during the discharge.

The guided discharge was imaged with the help of a 16-bit intensified charge-coupled device camera (ICCD) operated with a gate opening time of 100 ns. Examples of ICCD images for different delays in the range of $\tau = 15$–$130\,\mu$s are presented in Fig. 3. A dilatation factor of $Y/X \approx 4$ has been used to present ICCD images for a better visibility of the plasma cross section. An integrated image of the discharge is also presented to show the electrode geometry (Fig. 3(d)). This series of instantaneous images reveals that the guided discharge conserves the same linear shape during the whole life of the discharge, up to 130 μs. One should also note that the plasma is brighter close to the Marx electrode.

Reuse of AIP Publishing content is subject to the terms at: https://publishing.aip.org/authors/rights-and-permissions. Download to IP: 134.157.80.70 On: Mon, 09 May 2016 08:45:08

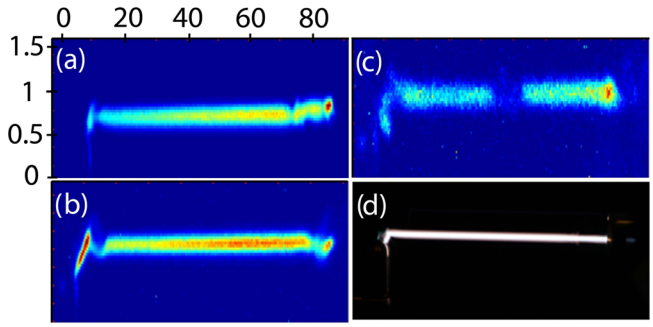

FIG. 3. ICCD images of the guided discharge taken at a delay $\tau = 15\,\mu s$ (a), $60\,\mu s$ (b), and $130\,\mu s$ (c) and time integrated image of the guided discharge (d). The spatial scale is indicated in mm and intensity color scale is normalized. The Marx generator is on the right side, and the laser beam comes from the left.

Fig. 4(a) shows a typical transverse luminosity profile integrated over 15 mm. To analyze the temporal evolution of the plasma channel while minimizing artifacts due to discontinuities, we integrated the luminosity profile with a threshold defined as the half maximum of the luminosity profile. Fig. 4(b) shows the temporal evolution of the integrated discharge luminosity measured at each maxima of discharge current. The points are well fitted by an exponential curve with a decay time constant of $24\,\mu s$ (red curve). It is worth noting that the current decay time is almost two times longer, with a value of $42\,\mu s$. It is an indication that the total light luminosity is proportional to the square of the current. On should note that with a higher temporal resolution, the plasma luminosity should present an oscillating decay similar to the square of the current signal.

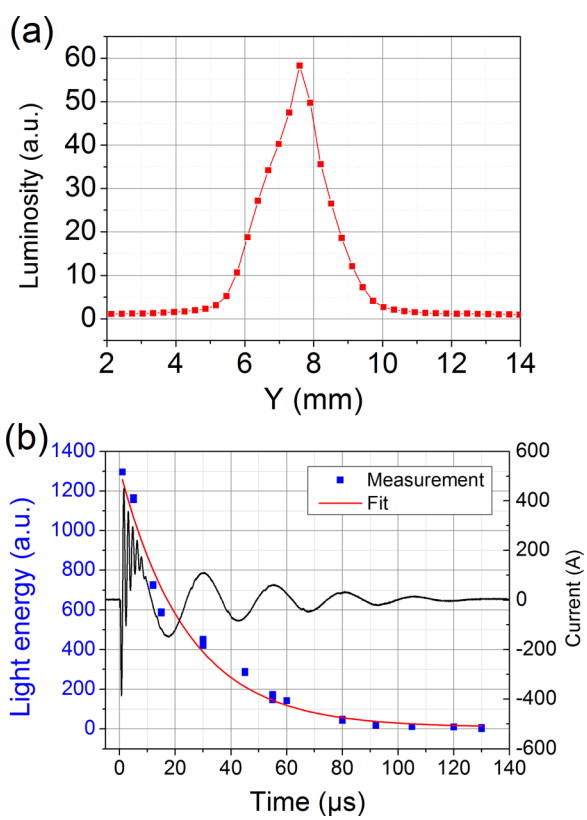

FIG. 4. (a) Plasma transverse luminosity profile measured by the ICCD camera and averaged over a 15 mm length. (b) Temporal evolution of the integrated discharge luminosity (blue squares) and the current signal (black line) measured in the oscillating regime ($R = 10\,\Omega$). The results are well approximated by an exponential decay fit with a constant of $24\,\mu s$ (red line).

The treatment described above allows us to control numerically the geometrical form of the guided discharge. We observe ICCD images with different percentage of guidance (70%–100%). As illustrated in Fig. 5; in some cases, the guided discharge presents discontinuities that we attribute to "jumps" of the initial current from one filament to the other. Similar discontinuities were observed in the guided discharges produced in our spark gap, Marx and Tesla experiments.[9,12,14,18] The average FWHM measured on the homogeneous parts of the images changes very weakly during $130\,\mu s$ with a value of 2.1 ± 0.2 mm.

The same measurements have been carried out in a damped current regime when a ballast resistance $R_2 = 100\,\Omega$ close to the circuit impedance was used. In this case with a positive polarization (see Fig. 6(a)), one observe two short current peaks ($\sim$0.5 and $1.5\,\mu s$) with amplitudes of -500 and 165 A followed by a relatively long tail with a maximum about 75 A.

Figs. 6(b) and 6(c) present the ICCD images taken at times $\tau = 1\,\mu s$, $14\,\mu s$, and $20\,\mu s$ in the case of damped regime. The luminosity behavior is very different from the oscillating regime. It presents a rapid drop in the first $4\,\mu s$ followed by a relatively slow evolution. It is interesting to note that the evolution of the plasma width in this regime is also significantly different. Its value decreases from 1.9–2.0 mm at the current beginning to 1.6 mm at its end ($\tau = 20\,\mu s$) when the current becomes close to zero (Fig. 6(d)).

In conclusion, we have increased the lifetime of a laser guided discharge up to $130\,\mu s$ by injecting a secondary current with a 20 kV charged additional circuit. The guided discharge was produced in atmospheric air by shorting an inter-electrode gap 85 mm with the help of a compact 100 kV Marx generator triggered by femtosecond laser source. We have measured a discharge resistance of $\sim$10–20 Ω, mostly due to contact processes in the vicinity of the electrodes. This result is promising for the development of plasma antenna, where electric circuit could be used in conjunction with intense ultra-short laser working at a kHz repetition rate[20] to realize a quasi-permanent plasma column.

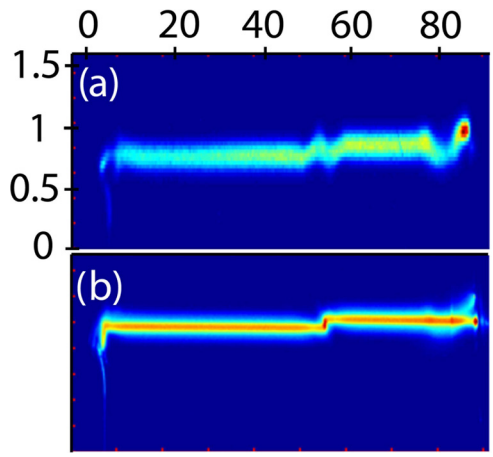

FIG. 5. Current "jump" event imaged by the ICCD at $\tau = 45\,\mu s$ (a) and corresponding time integrated picture (b).

Reuse of AIP Publishing content is subject to the terms at: https://publishing.aip.org/authors/rights-and-permissions. Download to IP: 134.157.80.70 On: Mon, 09 May 2016 08:45:08

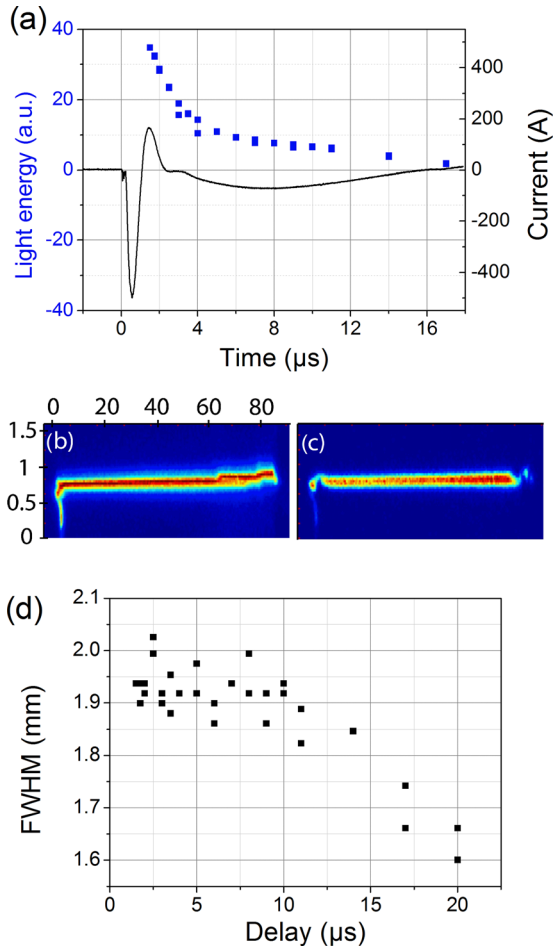

FIG. 6. (a) Temporal evolution of the light emission of the discharge (blue squares) and the current signal (black line) measured in the damped regime. (b) and (c) ICCD images taken at $\tau = 14$ and $20\,\mu s$ in the case of damped oscillations. (d) Average full width at half maximum of ICCD image profiles as a function of time. Resistance $R_2 = 100\,\Omega$.

Finally, the guided discharge remains straight up to $130\,\mu s$. This surprising result might be due to the mechanism of suppression of turbulent decay exposed by Leonov *et al.* in Ref. 21 or by the generation of the low density channel by the laser filament during the triggering of the discharge.[22,23] In a next step, we will try to increase the guided discharge duration up to the millisecond range and investigate further the physical mechanism and the limitation of this long time-scale guiding effect.

This project has been supported by the French Direction Generale de l'Armement (Grant No. 2013.95.0901). The authors acknowledge technical support by Jérôme Carbonnel, Yves-Bernard André, and Jean-Lou Charles and fruitful discussions with M. Pellet, S. Flajolet, and B. Larbi.

[1]A. Couairon and A. Mysyrowicz, Phys. Rep. **441**, 47 (2007).
[2]H. Pepin, D. Comtois, F. Vidal, C. Y. Chien, A. Desparois, T. W. Johnston, J. C. Kieffer, B. La Fontaine, F. Martin, F. A. M. Rizk, C. Potvin, P. Couture, H. P. Mercure, A. Bondiou-Clergerie, P. Lalande, and I. Gallimberti, Phys. Plasmas **8**, 2532 (2001).
[3]M. Rodriguez, R. Sauerbrey, H. Wille, L. Wöste, T. Fujii, Y.-B. André, A. Mysyrowicz, L. Klingbeil, K. Rethmeier, W. Kalkner, J. Kasparian, E. Salmon, J. Yu, and J.-P. Wolf, Opt. Lett. **27**, 772 (2002).
[4]B. Forestier, A. Houard, I. Revel, M. Durand, Y. B. André, B. Prade, A. Jarnac, J. Carbonnel, M. Le Nevé, J. C. de Miscault, B. Esmiller, D. Chapuis, and A. Mysyrowicz, AIP Adv. **2**, 012151 (2012).
[5]M. Henriksson, J.-F. Daigle, F. Théberge, M. Châteauneuf, and J. Dubois, Opt. Express **20**, 12721 (2012).
[6]J.-F. Daigle, F. Théberge, P. Lassonde, J.-C. Kieffer, T. Fujii, J. Fortin, M. Châteauneuf, and J. Dubois, Appl. Phys. Lett. **103**, 184101 (2013).
[7]F. Vidal, D. Comtois, C. Ching-Yuan, A. Desparois, B. La Fontaine, T. W. Johnston, J. Kieffer, H. P. Mercure, H. Pepin, and F. A. Rizk, IEEE Trans. Plasma Sci. **28**, 418 (2000).
[8]S. Tzortzakis, B. Prade, M. Franco, A. Mysyrowicz, S. Hüller, and P. Mora, Phys. Rev. E **64**, 57401 (2001).
[9]G. Point, Y. Brelet, L. Arantchouk, J. Carbonnel, B. Prade, A. Mysyrowicz, and A. Houard, Rev. Sci. Instrum. **85**, 123101 (2014).
[10]J. Kasparian, R. Ackermann, Y.-B. André, G. Méchain, G. Méjean, B. Prade, P. Rohwetter, E. Salmon, K. Stelmaszczyk, J. Yu, A. Mysyrowicz, R. Sauerbrey, L. Wöste, and J.-P. Wolf, Opt. Express **16**, 5757 (2008).
[11]T. Fujii, M. Miki, N. Goto, A. Zhidkov, T. Fukuchi, Y. Oishi, and K. Nemoto, Phys. Plasmas **15**, 013107 (2008).
[12]L. Arantchouk, A. Houard, Y. Brelet, J. Carbonnel, J. Larour, Y.-B. André, and A. Mysyrowicz, Appl. Phys. Lett. **102**, 163502 (2013).
[13]T. J. Dwyer, J. R. Greig, D. P. Murphy, J. M. Perin, R. E. Pechacek, and M. Raleigh, IEEE Trans. Antennas Propag. **AP–32**, 141 (1984).
[14]Y. Brelet, A. Houard, L. Arantchouk, B. Forestier, Y. Liu, B. Prade, J. Carbonnel, Y.-B. André, and A. Mysyrowicz, Appl. Phys. Lett. **100**, 181112 (2012).
[15]Z. Q. Hao, J. Zhang, Y. T. Li, X. Lu, X. H. Yuan, Z. Y. Zheng, Z. H. Wang, W. J. Ling, and Z. Y. Wei, Appl. Phys. B **80**, 627–630 (2005).
[16]B. Zhou, S. Akturk, B. Prade, Y.-B. André, A. Houard, Y. Liu, M. Franco, C. D'Amico, E. Salmon, Z.-Q. Hao, N. Lascoux, and A. Mysyrowicz, Opt. Express **17**, 11450 (2009).
[17]P. Polynkin and J. V. Moloney, Appl. Phys. Lett. **99**, 151103 (2011).
[18]L. Arantchouk, G. Point, Y. Brelet, J. Larour, J. Carbonnel, Y.-B. André, A. Mysyrowicz, and A. Houard, Appl. Phys. Lett. **104**, 103506 (2014).
[19]G. Point, Y. Brelet, A. Houard, V. Jukna, C. Milián, J. Carbonnel, Y. Liu, A. Couairon, and A. Mysyrowicz, Phys. Rev. Lett. **112**, 223902 (2014).
[20]A. Houard, V. Jukna, G. Point, Y.-B. André, S. Klingebiel, M. Schultze, K. Michel, T. Metzger, and A. Mysyrowicz, Opt. Express **24**, 7437 (2016).
[21]S. V. Leonov, Y. I. Isaenkov, and M. N. Shneider, Phys. Plasmas **14**, 123504 (2007).
[22]G. Point, C. Milián, A. Couairon, A. Mysyrowicz, and A. Houard, J. Phys. B **48**, 094009 (2015).
[23]G. Point, E. Thouin, A. Mysyrowicz, and A. Houard, Opt. Express **24**, 6271 (2016).

Reuse of AIP Publishing content is subject to the terms at: https://publishing.aip.org/authors/rights-and-permissions. Download to IP: 134.157.80.70 On: Mon, 09 May 2016 08:45:08